Mod Pathol 37 (2024) 100475

MODERN PATHOLOGY

USCAP UNITED STATES AND CANADIAN ACADEMY OF PATHOLOGY
Creating a Better Pathologist

Journal homepage: https://modernpathology.org/

Research Article

Primary Cilia as a Tumor Marker in Pituitary Neuroendocrine Tumors

Rebeca Martínez-Hernández[a,*], Ana Serrano-Somavilla[a], Raul Fernández-Contreras[a], Cristina Sanchez-Guerrero[a], Nuria Sánchez de la Blanca[a], Pablo Sacristán-Gómez[a], Fernando Sebastian-Valles[a], Miguel Sampedro-Núñez[a], Javier Fraga[b], María Calatayud[c], Almudena Vicente[d], Gonzalo García-de-Casasola[e], Ancor Sanz-García[f], Marta Araujo-Castro[g], Ignacio Ruz-Caracuel[h], Manel Puig-Domingo[i], Mónica Marazuela[a,*]

[a] *Department of Endocrinology and Nutrition Hospital Universitario de la Princesa, Instituto de Investigación Sanitaria Princesa, Universidad Autónoma de Madrid, and Centro de Investigación Biomédica en Red de Enfermedades Raras (CIBERER GCV14/ER/12), Madrid, Spain;* [b] *Department of Pathology, Hospital Universitario de la Princesa, Instituto de Investigación Sanitaria Princesa, Universidad Autónoma de Madrid, Madrid, Spain;* [c] *Department of Endocrinology and Nutrition, Hospital Universitario 12 de Octubre, Madrid, Spain;* [d] *Department of Endocrinology and Nutrition, Hospital Universitario de Toledo, Toledo, Castilla-La Mancha, Spain;* [e] *Department of Pathology, Hospital Universitario Infanta Cristina, Parla, Madrid, Spain;* [f] *Faculty of Health Sciences, Universidad de Castilla la Mancha, Talavera de la Reina, Castilla-La Mancha, Spain;* [g] *Department of Endocrinology, IRYCIS, CIBERONC, Madrid, Spain;* [h] *Department of Pathology Hospital Ramon y Cajal, IRYCIS, CIBERONC, Madrid, Spain;* [i] *Department of Endocrinology and Nutrition, Department of Medicine, Germans Trias i Pujol Research Institute and Hospital, Universitat Autònoma de Barcelona, Badalona, Spain and Centro de Investigación Biomédica en Red de Enfermedades Raras CIBERER G747, Madrid, Spain*

ARTICLE INFO

Article history:
Received 31 August 2023
Revised 6 March 2024
Accepted 10 March 2024
Available online 19 March 2024

Keywords:
ciliogenesis
pituitary neuroendocrine tumors
primary cilia
tumor marker

ABSTRACT

Pituitary neuroendocrine tumors (PitNETs) account for approximately 15% of all intracranial neoplasms. Although they usually appear to be benign, some tumors display worse behavior, displaying rapid growth, invasion, refractoriness to treatment, and recurrence. Increasing evidence supports the role of primary cilia (PC) in regulating cancer development. Here, we showed that PC are significantly increased in PitNETs and are associated with increased tumor invasion and recurrence. Serial electron micrographs of PITNETs demonstrated different ciliation phenotypes (dot-like versus normal-like cilia) that represented PC at different stages of ciliogenesis. Molecular findings demonstrated that 123 ciliary-associated genes (eg, *doublecortin domain containing protein 2, Sintaxin-3, and centriolar coiled-coil protein 110*) were dysregulated in PitNETs, representing the upregulation of markers at different stages of intracellular ciliogenesis. Our results demonstrate, for the first time, that ciliogenesis is increased in PitNETs, suggesting that this process might be used as a potential target for therapy in the future.

Introduction

Pituitary adenomas or, more recently, pituitary neuroendocrine tumors (PitNETs) are monoclonal tumors arising from the neuroendocrine epithelial cells of the adenohypophysis, which represent more than 10% of all intracranial neoplasms.[1,2] These tumors are classified according to their function as either functional or nonfunctional adenomas (NF-PitNETs). Functional adenomas can result in distinct hypersecretory syndromes, depending on the cell type. Corticotrophic tumors cause Cushing disease, somatotrophic tumors cause acromegaly, prolactin (PRL)-secreting tumors cause hyperprolactinemia, and thyrotropin-secreting tumors cause hyperthyroidism. In contrast, the diagnosis of NF-PitNETs is clinically challenging because they do not produce a hormonal hypersecretion

* Corresponding authors.
E-mail addresses: rebeca.martinez@salud.madrid.org (R. Martínez-Hernández), monica.marazuela@salud.madrid.org (M. Marazuela).

https://doi.org/10.1016/j.modpat.2024.100475

syndrome and are usually diagnosed either incidentally or in relation to local compressive symptoms such as headache and visual field defects.[3] Gonadotroph tumors can cause hypogonadism; however, they usually appear nonfunctioning and present with an incidental sellar mass.[4] According to the new "2022 World Health Organization Classification of Pituitary Tumors," PitNETs can be classified according to the cell type and lineage-specific transcription factors (TFs). The classification includes tumors from the PIT-1 lineage (eg, somatotroph, lactotroph, mammosomatotroph, thyrotroph, mature plurihormonal, immature, acidophil stem cell, mixed somatotroph, and lactotroph tumors), T-PIT lineage (eg, corticotroph), SF-1 lineage (eg, gonadotroph), plurihormonal (expressing multiple hormones, with no distinct cell lineage), null cell (expressing neither hormones nor TFs), and other under-represented PitNETs.[5] The first-line treatment for most tumors (except for prolactinomas) includes transnasal/transsphenoidal surgical resection.[6] Although the pathogenic mechanisms underlying pituitary tumorigenesis remain unknown, different molecular mechanisms, including genetic and epigenetic changes, have been associated with pituitary neoplasia initiation.[7,8] Although these tumors are usually benign, a small percentage occasionally exhibit worse behavior with rapid growth, tumor invasion, refractoriness to treatment (eg, medical therapy, surgery, or radiotherapy), and/or recurrence after therapy.[9,10] Several molecular markers, such as E-cadherin[11] and vascular endothelial growth factor,[12] as well as mutations in *aryl hydrocarbon receptor-interacting protein* (*AIP*),[13] *menin1*,[14] *G protein-coupled receptor 101*,[15] and alpha thalassemia/mental retardation syndrome X-linked,[16] among others[8] have been described to influence tumorigenesis behavior and/or response to therapy.[9,10,17,18]

Primary cilia (PC) are antenna-like organelles that project from the cell membrane to the extracellular environment and consist of a microtubule-based core structure that elongates from the basal body (BB).[19] PC are considered crucial sensors that provide the ability to fine-tune cell signaling and thus participate in key cellular processes. Malfunctioning cilia can cause a diverse set of diseases called ciliopathies. Recently, an emerging role for PC in the regulation of cancer development has been described.[20-22] PC function as a control center for various signaling pathways associated with tumorigenesis, including the Hedgehog,[23] Wnt,[24] and platelet-derived growth factor[25] signaling pathways. In addition, a close relationship between PC and the cell cycle has been reported.[20-22,26,27]

Cells from different endocrine organs possess PC that can colocalize with hormone receptors. Growing evidence has highlighted the association between these organelles and some endocrine-related cancers.[27,28] PC loss appears to be a consistent feature of several endocrine tumors including breast,[29] ovarian,[30] prostate,[31] and thyroid[32] cancers, although there is still a limited number of relatively small studies (reviewed in O'Toole and Chapple[27]). In the present study, we performed morphometric and ultrastructural analyses of PC from different types of PitNETs. Furthermore, using transcriptomic RNA-seq repository data, we performed a comparative analysis of ciliary signatures from different PitNETs. Interestingly, we demonstrated that a defect, excess, or imbalance in ciliogenesis might be involved in the development of these tumors.

Materials and Methods

Individuals

This retrospective study included consecutive patients with PitNETs with available tumor samples from 5 reference centers in Spain (Hospital Universitario La Princesa, Hospital 12 de Octubre, Hospital Cruces de Bilbao, Hospital Ramon y Cajal, and Hospital Virgen de la Salud) between 1996 and 2019. One hundred and seventeen patients with PitNETs and 14 normal pituitary glands from autopsy specimens were studied. All postmortem control pituitary tissues were obtained within 24 hours of death. The pituitaries have neither tumoral nor inflammatory pathologies nor ischemic changes. Pathological classification, imaging, and clinical phenotypic characteristics are shown in Supplementary Table S1. PitNETs were classified by expert endocrinologists and neurosurgeons according to functioning type (65 functioning and 52 nonfunctioning), tumor size (19 micro- and 98 macro-adenoma), cavernous sinus invasion according to Knosp grade (55 invasive [Knosp $\geq$3] and 47 noninvasive [Knosp <3)], and recurrence of the disease after surgery, defined as reappearance of disease (radiological and/or biochemical) at follow-up after complete surgical resection (13 with recurrence and 104 without recurrence). All tumors were classified according to the 2022 World Health Organization classification[33] as stated in the European Pituitary Pathology Group proposal.[34] This classification uses a combination of immunohistochemical assessments of adenohypophyseal hormone expression (growth hormone [GH], prolactin, follicle-stimulating hormone [FSH], luteinizing hormone [LH], thyroid-stimulating hormone [TSH], and adrenocorticotroph hormone [ACTH]), followed by pituitary TF expression (eg, PIT-1, SF1, T-Pit 19, and GATA3) in cases with limited or absent expression or unusual combinations of pituitary hormones.

This study was approved by the Ethics Committee of the Hospital de La Princesa, and written informed consent was obtained from all participants before inclusion, in accordance with the Declaration of Helsinki.

Tissue Samples

A total of 131 formalin-fixed paraffin-embedded tissues were evaluated using tissue microarray (TMA). Of these, 117 were tumor samples with a pathological diagnosis of PitNETs and 14 corresponded to healthy pituitary samples from autopsy specimens. All samples were duplicated in the same TMA and were collected and managed in accordance with local regulations with the approval of the local Ethics Institutional Board.

Immunofluorescence and Immunohistochemistry

TMA sections (4 μm) from PitNETs were placed in an oven at 65 °C for 30 minutes. Sections were deparaffinized in xylene and rehydrated using graded alcohol solutions. Antigen retrieval was performed in a PTLink instrument using the EnVision Flex target retrieval solution at high or low pH (Dako). For immunofluorescence, nonspecific binding was blocked using 5% bovine serum albumin and 10% normal goat serum for 30 minutes. Primary antibodies against ADP ribosylation factor-like GTPase 13B (Arl13B) (Proteintech Cat# 17711-1-AP, RRID:AB_2060867), GH (R and D Systems Cat# AF1067, RRID:AB_354573), PRL (Santa Cruz Biotechnology Cat# sc-46698, RRID:AB_628174), FSH (Ventana Medical Systems Cat# 760-2710, RRID:AB_2335963), ACTH (Santa Cruz Biotechnology Cat# sc-69648, RRID:AB_1118657), and LH (Ventana Medical Systems Cat# 760-2802 RRID:AB_2939029) were incubated overnight at 4 °C. The following day, an Alexa 488-labeled donkey antimouse (Thermo Fisher Scientific Cat# A32766, RRID:AB_2762823), an Alexa 568-labeled donkey antirabbit (Thermo Fisher Scientific Cat# A10042, RRID:AB_2534017), an

Alexa 488-labeled donkey antigoat (Thermo Fisher Scientific Cat# A-11055, RRID:AB_2534102), and an Alexa 647-labeled donkey antigoat (Thermo Fisher Scientific Cat# A-21447, RRID:AB_2535864) were used as secondary antibodies, and nuclei were counterstained with 4′,6-diamidino-2-phenylindole. For cilia quantification, high-resolution images were acquired from 5- to 7-μm-thick stacks using a Leica SP5 confocal microscope (Leica Microsystems). For immunohistochemistry of pituitary TFs, endogenous peroxidase was inhibited using a peroxidase-blocking solution (Dako) for 10 minutes. Afterward, sections were immunostained with the following antibodies: PIT-1 (Novus Cat# NBP1-92273, RRID:AB_11030310), GATA3 (Ventana Medical Systems Cat# 760-4897 RRID:AB_2905619), SF1 (Abcam, Cat# ab217317, RRID:AB_2920891), and T-Pit 19 (Novus, Cat# NBP2-61438, RRID:AB_2920892) overnight at 4 °C. Next, the sections and negative controls (without primary antibodies) were incubated with the appropriate horseradish peroxidase-conjugated secondary antibodies: goat antimouse (Agilent Cat# P0447, RRID:AB_2617137) or goat antirabbit (Agilent Cat# P0448, RRID:AB_2617138). Finally, the sections were incubated with 3,3′-diaminobenzidine (Dako), counterstained with hematoxylin (Sigma-Aldrich), dehydrated in alcohol, cleared with xylene, and mounted.

Morphometric Analysis of Primary Cilia

The frequency of cilia was estimated manually by analyzing Z-stacked images using a confocal microscope. For each tissue, all TMA areas were analyzed by 2 independent observers in a blinded manner at a higher magnification resolution. The frequency of ciliated cells was estimated using a cilia index (CI) score. CI was assigned according to the cilia length (categorized as dot-like cilia and normal-like cilia) and the percentage of ciliated area on the TMA tissue (categorized as ~25%, ~50%, ~75%, and >75% of ciliated cells). The CI was quantified according to a scale of 1 to 13, as detailed in Supplementary Figure S1, and values were obtained using the mean of 4 values (2 viewers per 2 duplicated samples).

Transmission Electron Microscopy

An ultrastructural study of the PC using electron microscopy was performed in 6 patients. Patient #1 was diagnosed with a somatotrophic tumor positive for Pit1, GH, and sparse PRL with a Ki67 <3%. Patient #2 was NF-PitNET-positive for Pit1 and PRL, with a Ki67 <3%. Patient #3 was diagnosed with Cushing disease and was positive for ACTH and had a Ki67 <3%. Patient #4 was NF-PitNET-negative for all hormones and TFs, with a Ki67 = 3%. Patient #5 was NF-PitNET-positive for FSH, LH, SF1, and GATA3, with a KI67 <3%. Patient #6 had a TSH-secreting tumor positive for Pit1, sparse SF1, with <3% focal expression of TSH, PRL, and Ki67.

Fresh pituitary slices were fixed in 2.5% glutaraldehyde in 0.1 M PB, pH 7.4, for 2 hours at room temperature and overnight at 4 °C. The samples were postfixed in 1% osmium tetroxide for 1 hour at 4 °C, block-stained with 2% uranyl acetate, dehydrated, and then embedded in epoxy Resin TAAB 812 (TAAB laboratories). Semi-thin sections (1 μm) were cut on an ultramicrotome and stained with toluidine blue. Ten to 15 serial ultrathin sections (60 to 80 nm) were obtained from the selected areas, counterstained with 2% uranyl acetate and lead citrate, and observed using a JEM1400 Flash (Jeol) electron microscope. Pictures were captured using a CMOS 4K × 4K digital camera (Gatan OneView; Gatan).

Western Blot and Antibodies

Pituitary tissue samples from 4 somatotrophs, 4 NF-PitNETs, and 3 healthy controls were disaggregated and resuspended in radio-immunoprecipitation assay buffer (Sigma-Aldrich) containing a protease inhibitor (HaltTM, Thermo Fisher Scientific). After 30 minutes on ice, the samples were sonicated, the lysates were centrifuged at 12,700 rpm for 10 minutes, and the supernatants were collected. Western blots were performed using 4% to 15% 12-well precast protein gels (Mini-PROTEAN TGX). Protein homogenates were lysed in Laemmli buffer, and the membranes were probed with rabbit polyclonal antisera against Arl13B (Proteintech Cat# 17711-1-AP, RRID:AB_2060867) or β-actin (Santa Cruz Biotechnology Cat# sc-47778, RRID: AB_626632). Immunolabeling was detected using enhanced chemiluminescence (SuperSignal West Femto Maximum Sensitivity Substrate, Thermo Scientific) and visualized using a digital luminescent image analyzer (ImageQuant LAS400 mini).

Transcriptome In Silico Analysis

For transcriptome in silico analysis, a microarray data set from the Gene Expression Omnibus (GEO; accession number: GSE63357)[35] and RNA-seq data from the European Bioinformatics Institute (accession number: E-MTAB-7768)[36] were downloaded. From the microarray data, 3 sporadic somatotropinomas, 4 sporadic NF-PAs, and 5 normal glands were analyzed. Briefly, a $\log_2$ transformation was applied to all samples (excluding failed samples). In the case of more than one probe per gene, all probe sets were collapsed by calculating the mean expression. The data were grouped and categorized using principal component analysis to identify possible outliers. For differential expression between the groups, empirical Bayesian methods were applied using the Limma methodology. A fold-change threshold of 2 and a *P* value adjusted using a false discovery rate of .05 were used for gene selection. Functional enrichment analysis of differential gene expression was performed using clusterProfiler v3.18.1,[37] with a threshold *P* value adjusted using an false discovery rate of .05. We selected all statistically significant categories present in the GO,[38] the KEGG,[39] and REACTOME[40] databases.

Data Analysis

To assess the discriminant potency of the CI score, the patients were randomly assigned to 2 cohorts to ensure the same proportion of outcomes in both cohorts. The first cohort (two-thirds of all patients) was used to derive the weights of the score components from the logistic regression algorithm, and the second cohort (one-third of all patients) was used as the validation cohort. The discriminant validity of the CI was assessed using the area under the receiver operating characteristic curve, and the specificity, sensitivity, positive predictive value, negative predictive value, positive likelihood ratio, and negative likelihood ratio of the CI were also calculated. The optimal cutoff value to determine high-risk groups, specificity, and sensitivity was assessed using the Youden index. The patient data presented completely missing values at random. The strategy used to handle missing data (listwise deletion) did not include biased means, variances, or regression weights.

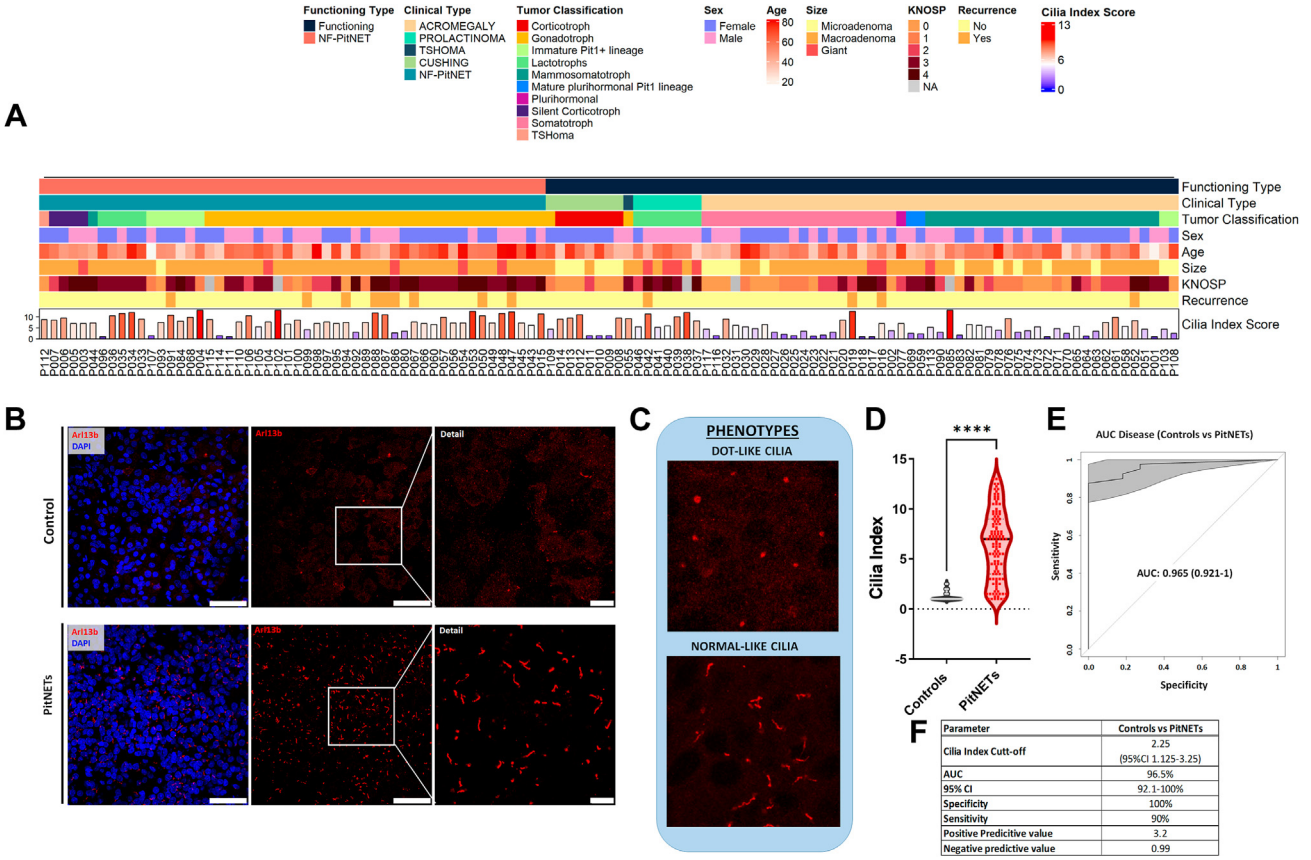

Figure 1.
Cilia patterning in pituitary neuroendocrine tumors (PitNETs) and in healthy pituitary. Clinical and pathological characteristics of PitNET patients (A). Representative images captured using confocal microscopy characterizing the primary cilia (PC) of controls and PitNETs stained with Arl13b (in red) and nuclei counterstained with 4′,6-diamidino-2-phenylindole (DAPI; blue). Scale bar = 50 μm and 10 μm (B). Representative images of the different phenotypes found in PitNET tissues: dot-like and normal cilia (C). Violin plot displaying the quantification of PC using the cilia index score, as reported in the Material and Methods section (D). Receiver operating characteristic (ROC) curve analyses performed to assess the diagnostic value of CI to discriminate between healthy subjects and patients (controls vs PitNETs) (E). The table shows values of cutoff, area under the curve (AUC), 95% CIs, sensitivity, and specificity of the ROC curve analyses for CI (F). Data correspond to the median (line within violin). Differences were analyzed using the Mann-Whitney test. ns, not significant; ****$P < .001$.

Statistical Analysis

Quantitative variables were expressed as medians and IQRs (box and whisker plots). The Mann-Whitney U test was used to compare 2 independent groups, and one-way analysis of variance was used to compare more than 2 groups. Post hoc multiple comparisons were performed using Tukey's test. Spearman's rho analysis was performed to detect correlations between the markers examined by immunofluorescence. Samples from all groups within an experiment were processed simultaneously. The P values were 2-sided, and statistical significance was considered at $P < .05$. Data are presented with the specific P values: * = $P < .05$, ** = $P < .01$, *** = $P < .005$, and **** = $P < .001$. All statistical analyses were performed using GraphPad Prism 4 and R v 3.5.1 software.

Results

Ciliogenesis Is Upregulated in Pituitary Neuroendocrine Tumors

A total of 117 patients were included in the analysis, comprising 66 females and 51 males with a median age of 56 and 51 years, respectively ($P = .11$). These PitNETs included 49 patients with acromegaly, 8 with Cushing disease, 52 with nonfunctioning (NF) PitNETs, 7 with prolactinomas, and 1 with TSHoma. Regarding pathological classification, the tumors consisted of 20 somatotrophs, 12 lactotrophs, 25 mammosomatotrophs, 37 gonadotrophs, 7 corticotrophs, 4 silent corticotrophs, 1 TSHoma, 8 immature Pit1+ lineages, 2 mature plurihomornal lineages, and 1 plurihormonal (Fig. 1A).

We analyzed control pituitary samples by triple immunofluorescence for the different hormones (eg, GH, PRL, ACTH, FSH, and LH) co-stained with Arl13B, a marker specific for ciliary membrane Arl13b. We performed a morphometric analysis examining PC according to their appearance (cilia length: normal-like and very short or dot-like) and frequency, as described in the Materials and Methods section (Supplementary Fig. S1). In controls, PC was scant, with a very low Arl13b signal in the scattered cells (Figs. 1B and 2A). A significant increase in CI was observed in PitNETs, compared with control pituitary glands (CI: 6.4 ± 3.4 vs 1.23 ± 0.45; $P < .001$, Fig. 1B, C). Using Youden's index, we determined the optimal cutoff value for CI to differentiate healthy controls from patients with PitNET, and the best CI cutoff for disease discrimination was 2.25. Receiver operating characteristic curve analyses for these cutoffs suggested that CI was a good discriminator between patients with PitNETs and

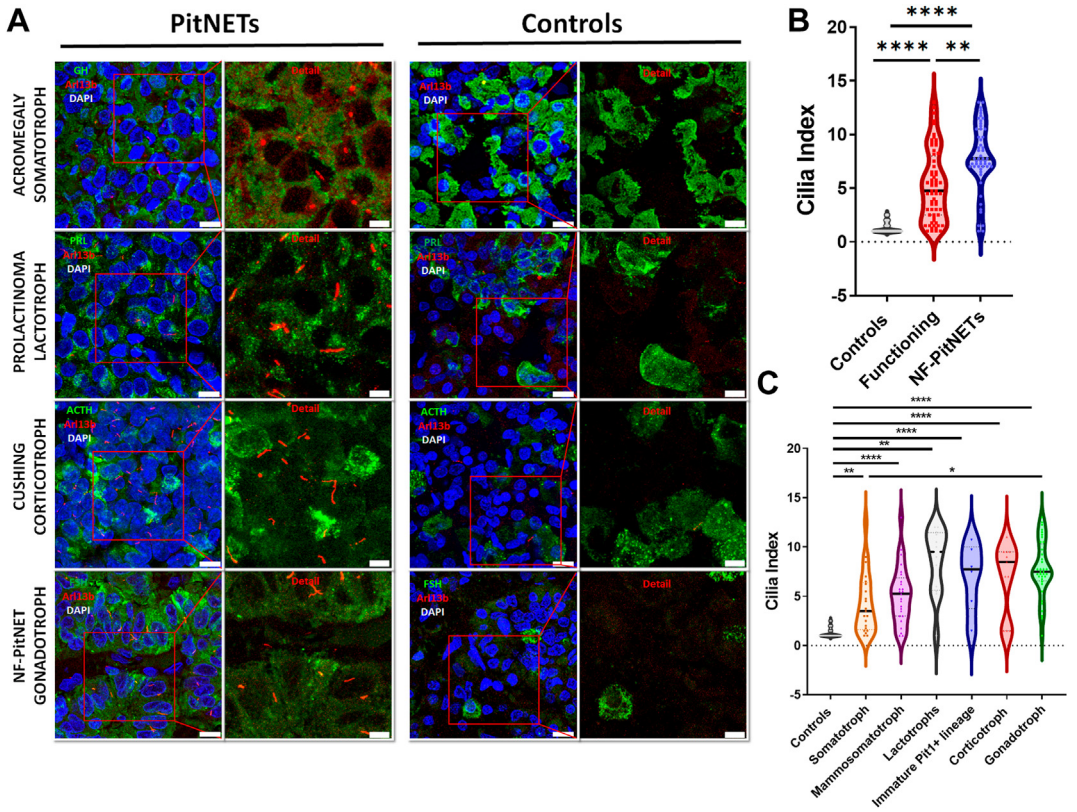

Figure 2.
Cilia patterning of the different tumor types compared with controls. Representative images of double immunofluorescence staining for growth hormone (GH), prolactin (PRL), adrenocorticotroph hormone (ACTH), and follicle-stimulating (FSH; in green) and Arl13b (in red) in different pituitary neuroendocrine tumors (PitNETs) and in controls. Scale bar = 50 μm and 10 μm (A). Box plots representing cilia index in the different types of PitNETs: Functioning versus nonfunctional pituitary neuroendocrine tumors (NF-PitNETs) (B) according to their pathological classification (C). Data corresponding to the median (lines within violins). Differences were analyzed using the Kruskal–Wallis test. *$P < .05$; **$P < .01$; ***$P < .005$; ****$P < .001$.

healthy donors, with an area under the curve of 0.965, a specificity of 100%, and a sensitivity of 90% (Fig. 1D). Arl13b expression was also assessed in pituitary protein extracts using western blotting. We confirmed a significant increase in this marker in PitNETs compared with controls ($P < .001$) (Supplementary Fig. S2).

Different Phenotypes of Primary Cilia Are Found in Different Pituitary Neuroendocrine Tumors

We then evaluated the frequency of PC according to different PitNET tumor types. Interestingly, double immunofluorescence studies of pituitary hormones and Arl13b showed that all tumor cells from each histological type had PC, unlike the controls (Fig. 2A). When we evaluated the cilia patterning of PitNETs according to their clinical functionality, we found that the CI was significantly higher in NF-PitNETs than in functional tumors (7.88 ± 3.1 vs 5.3 ± 3.3, respectively, $P = .002$, Fig. 2B). To further explore the differences between ciliated cells in different tumors, we analyzed CI according to their pathological classification (Fig. 2C). Interestingly, all PitNETs presented a significantly elevated CI compared with controls. Somatotroph tumors presented a significantly decreased CI when compared with gonadotrophs (4.3 ± 3.1 vs 7.8 ± 2.9, $P = .03$) with an increased percentage of dot-like cilia (Fig. 2A, C).

Ultrastructure of Primary Cilia

To further elucidate the ultrastructural morphology of PC in PitNETs, we performed conventional transmission electron microscopy (TEM). The biopsy tissues of 6 PitNETs (3 NF-PitNETs [1 silent prolactinoma, 1 hormone-negative, and 1 gonadotropinoma], 1 Cushing, 1 TSHoma, and 1 acromegaly) were analyzed using serial ultrathin sections. Ultrastructural characterization of tumor tissues showed heterogeneous patterns with different numbers and morphologies of secretory granules, prominent rough endoplasmic reticula, and Golgi complexes, as previously described (Supplementary Fig. S3).[41-43]

Interestingly, we found different stages of ciliogenesis in PITNETs, ranging from early stages formed only by BBs (ie, immature cilia) to fully formed PC (Fig. 3). Ultrastructurally, immature cilia are characterized by BBs composed of 9 peripheral microtubule doublets, forming a hollow cylindrical architecture surrounded by subdistal appendages. Above the transition zone of BBs, ciliary vesicles (CVs) were found attached to the distal appendages (Fig. 3, "Immature cilia"). Intracellular cilia showed microtubule-based axonemes starting at the BBs and forming an invagination corresponding to the ciliary pocket (CP). The axoneme remained inside the cell cytoplasm without reaching the cell membrane (Fig. 3, "Intracellular cilia"). In mature cilia, large axonemes were composed of parallel microtubules extending through the cytoplasm to the intercellular space outside the cell membrane (Fig. 3, "Extracellular cilia").

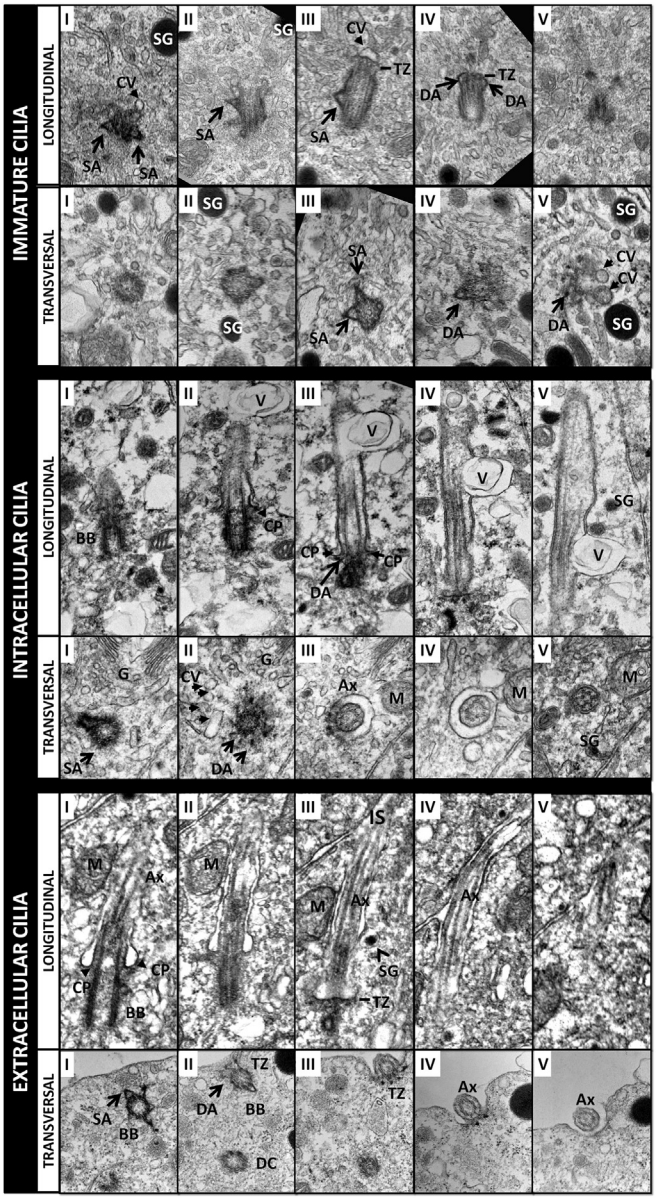

Figure 3.
Ultrastructure progressive changes of PC from serial sections of different PitNETs at longitudinal and transversal levels. Immature cilia: Longitudinal: A BB showing triangular SAs (arrows). A CV (arrowhead) is associated with the distal end above the TZ. Transversal: A BB showing SAs and DAs at different levels. In subsequent sections, CVs appear to be docking at the DAs. Intracellular cilia: Longitudinal: A docked BB with DAs anchoring to the ciliary pocket (CP). The axoneme extends though the cytoplasm without reaching the cell membrane. A large vesicle is shown next to the axoneme. Transversal: A PC showing the progressive changes from the proximal BB to the distal part of the cilium. SAs and DAs can be observed docking to the membrane. Microtubule doublets progressively shift toward the core of the axoneme at the ciliary tip. Extracellular cilia: Longitudinal: Serial sections show a BB extending an Ax to the IS. A clear ciliary pocket is seen at the TZ. A SG from the cell is aligned to the cell membrane opposed to the Ax. Transversal: Cross sections of a BB docking to the cellular membrane harboring the 9-fold configuration of microtubule triplets revealing the SAs, DAs, and the TZ and extending the Ax out of the cell. Ax, axoneme; TZ, transition zone; BB, basal body; DAs, distal appendages; SAs, subdistal appendages; CV, ciliary vesicle; CP, ciliary pocket; vesicle, V; CM, ciliary membrane; SG, secretory granules; M, mitochondria; IS, intercellular space; PC, primary cilia; PitNETs, pituitary neuroendocrine tumors.

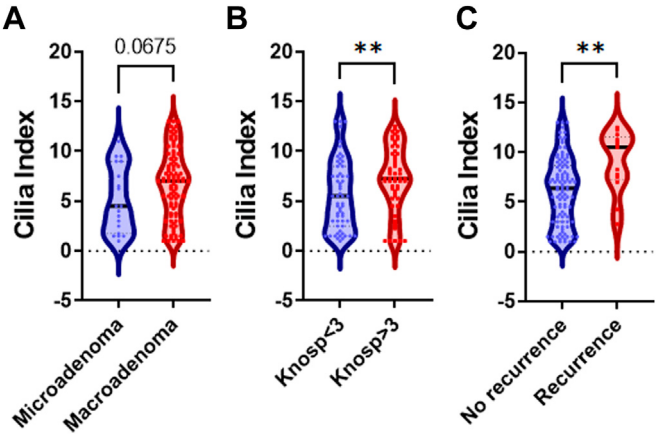

Figure 4.
Cilia are increased in invasive and recurrent pituitary neuroendocrine tumors (PiT-NETs). Cilia index was quantified and analyzed according to tumor size (microadenoma vs macroadenoma; A), degree of cavernous sinus invasion (Knosp <3 vs Knosp ≥3; B), and recurrence in PitNETs (C). Data correspond to the median (lines within violins). Differences were analyzed using the Mann-Whitney U test. ns, not significant; *$P < .05$; **$P < .01$; ***$P < .005$; ****$P < .001$.

Primary Cilia Are Associated With Invasion and Recurrence

Next, we evaluated the association between PC frequency in PitNETs and clinical behavior. The tumors were classified according to their size, Knosp grade, and disease recurrence (progression). Regarding tumor size, although differences were not statistically significant, there was a tendency toward an increase in PC in macroadenomas compared with microadenomas (mean CI, 5.1 ± 3.3 vs 6.7 ± 3.4, respectively; $P = .07$; Fig. 4A). Regarding the Knosp classification system, when we grouped tumors with Knosp ≥3, the CI exhibited a significant increase compared with Knosp <3 (7.3 ± 3.3 vs 5.6 ± 3.4; $P < .01$) (Fig. 4A). Moreover, CI was also significantly increased in recurring tumors (6.1 ± 3.6 vs 9 ± 3; $P < .01$, Fig. 4A).

Expression of Cilia-Associated Genes in Pituitary Neuroendocrine Tumors (Molecular Fingerprint of Ciliary-Associated Genes in Pituitary Neuroendocrine Tumors)

Our next approach was to identify ciliary molecular alterations involved in PitNETs by analyzing publicly available transcriptome data sets (GSE63357[35] used for data exploration and E-MTAB-7768[36] used as a validation data set). To elucidate the possible differences in the ciliary molecular fingerprint, we used 2 transcriptional signatures of cilia-associated genes (Supplementary Data S1).[44,45] First, we evaluated the ciliary genes that showed significant differential expression between controls, NF-PitNETs, and somatotroph-sporadic tumors (Fig. 5A, B). The results showed that 56 genes were upregulated in NF-PitNETs (eg, *doublecortin domain containing protein 2 (DCDC2), IFT122, TMEM231, CFAP20,* and *CEP41*, which are mainly involved in the formation and maintenance of cilia) and 27 genes were upregulated in sporadic somatotroph tumors (eg, *NME7, IQCG, NUP37,* and *TTC30A*, which are mainly involved in the regulation and maintenance of centrosomes and microtubules in the axonemes). The comparison between sporadic somatotrophs and NF-PitNETs revealed a total of 106 differentially expressed cilia-related

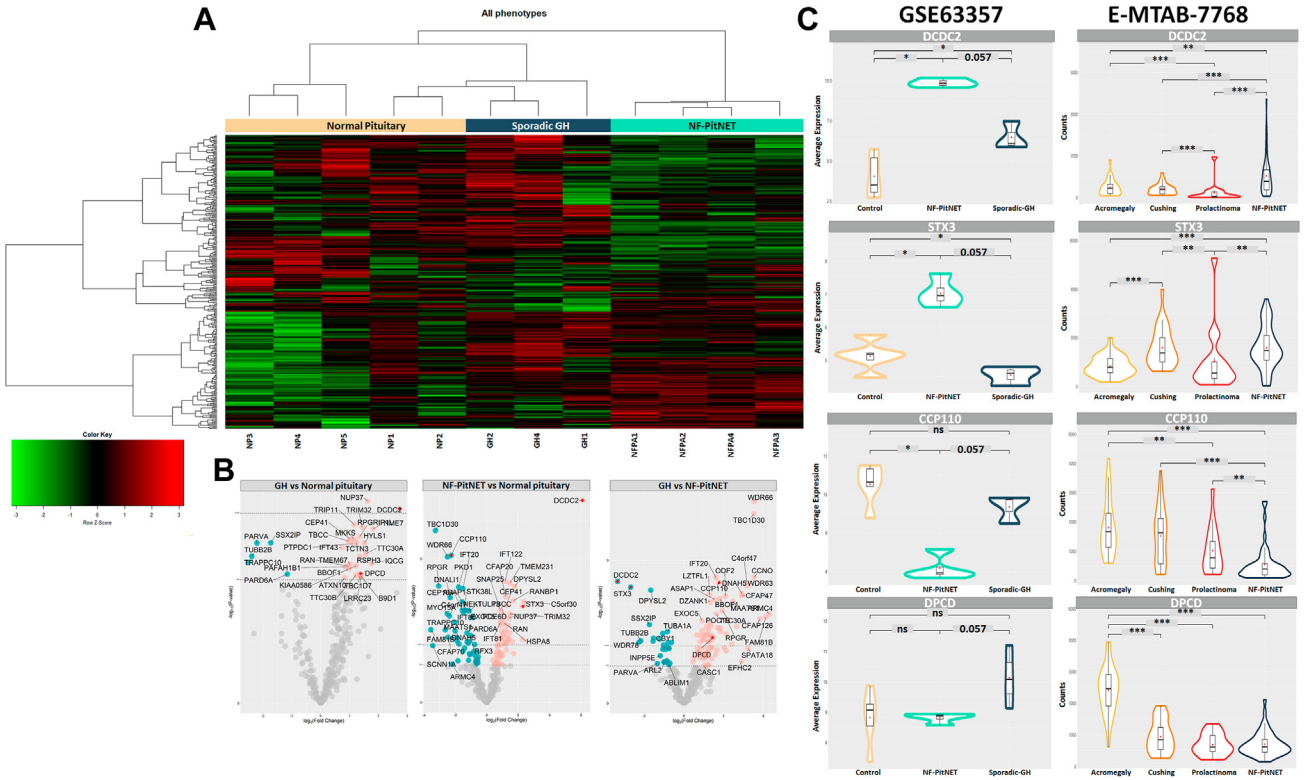

Figure 5.
Cilia-associated gene profiling in pituitary neuroendocrine tumors (PitNETs). Expression heatmap of the most differentially expressed (DEGs) ciliary-associated genes between groups (nonfunctional pituitary neuroendocrine tumors [NF-PitNETs], sporadic growth hormone [GH], and controls) from the data set downloaded from the Gene Expression Omnibus (GEO accession number: GSE63357)[35] (A). Volcano plots showing DEGs between the 3 groups (B). Violin plots showing the expression of *DCDC2*, *STX3*, *CCP110*, and *DPCD* in the different groups from 2 PitNET data sets, from GEO (GSE63357)[35] and from European Bioinformatics Institute (EMBL-EBI, accession number E-MTAB-7768)[36] (C).

genes (28 downregulated and 78 upregulated; Supplementary Data S2). The most upregulated gene commonly affected in both groups was the *DCDC2*; in NF-PitNETs, *Sintaxin-3* was at the top of the most overexpressed genes, whereas *centriolar coiled-coil protein 110* (*CCP110*, a centrosomal protein that suppresses ciliogenesis[46]) showed a significant decrease in expression in these tumors (Fig. 5B, C; Supplementary Fig. S4). In sporadic GH tumors, one of the most upregulated genes specific to this group was deleted of *primary ciliary dyskinesia gene* (*DPCD*) (Fig. 5C; Supplementary Figs. S4 and S5). To validate the expression of ciliary genes in different sample cohorts, we studied the profiles of these genes in different phenotypes of PitNETs using a different data set from E-MTAB-7768.[36] Interestingly, we found similar behavior in the ciliary expression profiles of acromegaly, prolactinomas, Cushing disease, and NF-PitNETs (Fig. 5C).

Discussion

Our morphometric and ultrastructural studies provided the first evidence that ciliogenesis, a key biological process in tumorigenesis, is altered in PitNETs. These tumors exhibit different types and numbers of PC at different stages of intracellular ciliogenesis (a schematic model of the different stages of intracellular ciliogenesis found in PitNETS is shown in Fig. 6). Moreover, the increase in cilia in PitNETs was associated with invasive and recurrent tumors, suggesting a possible role for these structures in tumor behavior.

Interestingly, we observed an increase in the number of cilia in PitNETs. PC can play opposing roles in cancer, either by promoting or preventing tumorigenesis, depending on the nature of the oncogenic initiating event.[22,47] Although only a limited number of studies have examined PC in tumors, in the majority of cancer types, including breast, prostate, renal, pancreatic, melanoma, cholangiocarcinoma, glioblastoma, chondrosarcoma, and colon tumors,[29,31,48-52] there is a reduction in cilia frequency relative to that in the adjacent normal tissue. However, some tumors, such as medulloblastoma and adamantinomatous craniopharyngioma, present with an increase in PC, likely reflecting changes in cilia-dependent signaling pathways.[27,53,54] Cilia dysfunction is probably an early event during the tumorigenic process and is more related to changes in the genes required for ciliogenesis than to altered cellular proliferation rates.[22] As PC can function as a tumor promoter, the characterization of the different types of PC highlights the potential of these structures to serve as biomarkers in PitNETs[26] and potentially as biomarkers of invasiveness.

Using immunofluorescence analysis, we also found different patterns of cilia (ranging from normal-like to dot-like), suggesting that defects in ciliogenesis may be present in PitNET tumors. To deepen our knowledge, we also performed ultrastructural studies on PitNETs using conventional TEM. Although there have been some previous ultrastructural studies on PitNETS,[41,42] this is the first time that the presence of PC has been reported in these tumors and compared with controls. In this context, only one study has described the presence of PC in normal pituitary follicular cells, but not in tumor cells from the human anterior pituitaries.[55]

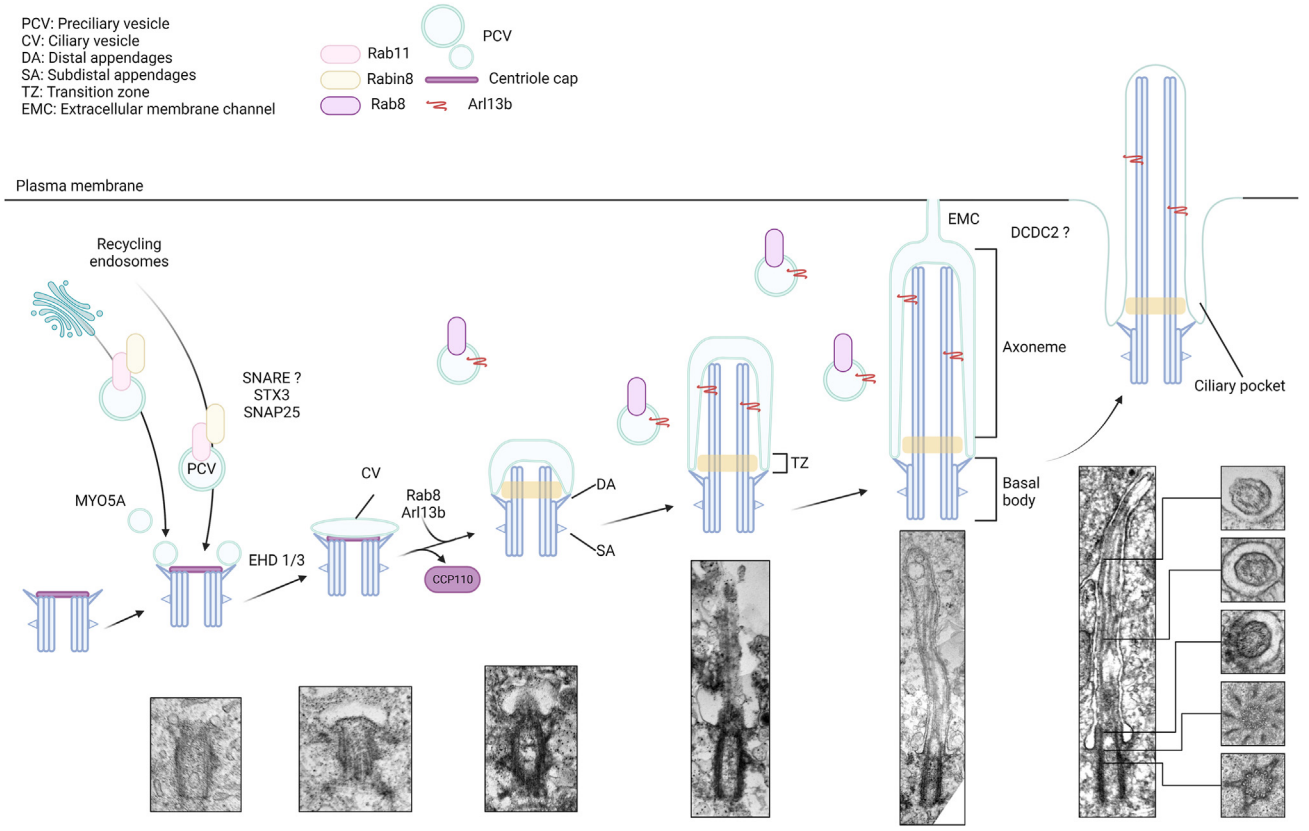

Figure 6.
Schematic stages of ciliogenesis in pituitary neuroendocrine tumors (PitNETs). Model of the different stages of intracellular ciliogenesis found in PitNETs, including key molecular steps. At the first steps, preciliary vesicles (CVs) associate with the distal appendages of the mother centriole. The assembly and fusion of CVs requires a SNARE complex in cooperation with SNAP25 and STX3. EHD1-3 proteins mediate the fusion to a larger vesicle. In the next steps, the ciliation inhibitor CCP110 is removed and Arl13b and Rab8 assemble to the ciliary membrane regulating the growth of the axoneme (adapted from Zhao et al and Breslow and Holland[56,57]).

This may be due to the challenge of finding these structures in TEM imaging, where they may be confused with other intracellular structures such as centrioles. Our serial section analysis by TEM allowed us to describe this structure in different tumor samples, identifying the presence of PC at different stages of ciliogenesis. Intracellular cilium formation is initiated by docking CVs to the distal appendages from the mother centriole.[56,57] The CVs then fuse and generate a CP membrane, followed by the extension of the axonemal microtubules, giving rise to a mature ciliary structure.[56] Phenotypes associated with a dot-like presence of PC in our immunofluorescence studies (mainly found in patients with acromegaly) could correspond to CVs surrounding and anchoring the BBs and could represent PC at the early stages of intracellular ciliogenesis (ie, immature and intracellular cilia). In this regard, TEM studies of glioblastoma tumor samples have also shown disrupted PC in the early stages of ciliogenesis.[51,58]

We observed different patterns of PC expression among the different histopathological groups of PITNETs. The greatest differences were found between nonfunctioning and somatotropic tumors. In this regard, our in silico molecular analysis showed increased expression of the *CCP110* gene in somatotrophs compared with NF-PitNETs. During multistep ciliogenesis, multiple protein complexes are involved in the recruitment of CVs and axoneme formation. In this regard, CCP110 is placed at the distal end of the centriole, and its removal is necessary to allow growth of the ciliary axoneme.[56,57] Moreover, there was an increase in *DCDC2* levels in PitNETs compared with controls. Interestingly, the overexpression of *DCDC2* has been associated with an increase in ciliary length and the activation of Sonic Hedgehog signaling in neurons.[59] Thus, it is plausible that the significant differences in the CI between somatotrophs and NF-PitNETs could be explained by different factors: (1) ciliogenesis in these samples is dysregulated, (2) the ciliogenesis process is dynamic, allowing the presence of PC at different stages, and (3) there is an arrest of ciliogenesis due to either the tumor type or the action of some treatment. In this regard, a deeper molecular analysis validating the expression of these genes in different tumors, as well as the effect of their treatment, is needed to assess their potential as future molecular biomarkers.

We correlated our results with clinical outcomes to assess the prognostic value of PC. We found that an increase in the number of cilia in PitNETs was associated with certain features related to prognosis, including cavernous sinus invasion and tumor recurrence after surgery. In other tumors, such as glioblastoma, an increase in ciliated cells has been related to an increase in invasion, aggressiveness, and treatment resistance.[51,52,58] Another study of bladder cancer reported the presence of PC in invasive cells, possibly explaining the high recurrence index of some of these tumors. Cilial elongation has also been associated with increased resistance to a variety of targeted therapies in cancer cells.[60] In these reports, drug resistance was associated with failure to control cilia length and cilia fragmentation. In this regard, it would be crucial to assess in a large cohort of samples the correlation

between different treatments and the number and pattern of cilia in order to provide evidence of the role of ciliogenesis in the refractoriness to treatments.

Overall, we suggest that cilia-dependent signaling pathways play a role in PitNET behavior. Although the classification of PitNETs has improved,[5,34,61,62] the definition of predictive markers for identifying tumors with worse behaviors is still lacking.[10,63] The identification of new markers could contribute to refining clinical decisions, improving postsurgical follow-up, and selecting more suitable therapies, including novel therapies that target ciliated PitNETs, and altogether, it could enable more personalized medicine in the future.

Conclusions

We provide the first analysis of PC in PitNETs and suggest that ciliogenesis is involved in tumorigenesis and progression of PitNETs.

Acknowledgments

We thank Francisca Molina-Jimenez from the Microscopy Unit of the Instituto Investigación de la Princesa (IISP) for technical assistance with confocal microscopy and Manuel Gómez for English corrections. We thank the Ramon y Cajal University Hospital IRYCIS Biobank for providing the tissue samples. We also thank Pedro Martínez Flórez and Jose Antonio Fernandez Alen from the Department of Neurosurgery at HUP for the sample acquisition. We also thank all the participants included in the study for their selfless participation.

Author Contributions

R.M.H., A.S.S., C.S.G., and P.S.G. conceived of and performed the experiments. R.M.H., A.S.S., R.F.C., N.S.B., M.S.N., and M.M. designed and interpreted the data. R.F.C., N.S.B., and A.S.G. developed the necessary computational and visualization tools. R.M.H., A.S.S., F.S.V., M.S.N., J.F., M.C., A.V., G.G.C., M.A.C., I.R.C., M.P.D., and M.M. collected the samples and contributed clinical and pathological expertise. R.M.H., A.S.S., M.P.D., and M.M. wrote the manuscript. All the authors critically reviewed the manuscript for important intellectual content and approved its final version.

Data Availability

The data sets used and/or analyzed in the current study are available from the corresponding author upon reasonable request.

Funding

This work was supported by the following grants: Proyectos de Investigación en Salud PI19/00584, PI22/01404 and PMP22/00021 (funded by Instituto de Salud Carlos III), iTIRONET—P2022/BMD7379 (funded by Comunidad de Madrid), Research project IPI/2022/N5 (funded by Sociedad de Endocrinología, Nutrición y Diabetes de la Comunidad de Madrid-SENDIMAD), and co-financed by FEDER funds to MM and RMH, as well as by Contratos Predoctorales de Formación en Investigación en Salud (FI20/00035 to PSG and FI23/00052 to NSB). The funders played no role in the study design, data collection, data analysis, interpretation, or writing of the report.

Declaration of Competing Interest

The authors declare that they have no competing interests.

Ethics Approval and Consent to Participate

This project was approved by the Internal Ethics Review Committee of the Hospital de La Princesa (reference number: 4783). Written informed consent was obtained from all participants prior to inclusion in accordance with the Declaration of Helsinki.

Supplementary Material

The online version contains supplementary material available at https://doi.org/10.1016/j.modpat.2024.100475

References

1. Herman V, Fagin J, Gonsky R, Kovacs K, Melmed S. Clonal origin of pituitary adenomas. *J Clin Endocrinol Metab*. 1990;71(6):1427–1433. https://doi.org/10.1210/jcem-71-6-1427
2. Melmed S. Pathogenesis of pituitary tumors. *Nat Rev Endocrinol*. 2011;7(5):257–266. https://doi.org/10.1038/nrendo.2011.40
3. Drummond J, Roncaroli F, Grossman AB, Korbonits M. Clinical and pathological aspects of silent pituitary adenomas. *J Clin Endocrinol Metab*. 2019;104(7):2473–2489. https://doi.org/10.1210/jc.2018-00688
4. Melmed S. Pituitary-tumor endocrinopathiesLongo DL, ed. *N Engl J Med*. 2020;382(10):937–950. https://doi.org/10.1056/NEJMra1810772
5. Asa SL, Mete O, Perry A, Osamura RY. Overview of the 2022 WHO classification of pituitary tumors. *Endocr Pathol*. 2022;33(1):6–26. https://doi.org/10.1007/s12022-022-09703-7
6. Molitch ME. Diagnosis and treatment of pituitary adenomas: a review. *JAMA*. 2017;317(5):516. https://doi.org/10.1001/jama.2016.19699
7. Caimari F, Korbonits M. Novel genetic causes of pituitary adenomas. *Clin Cancer Res*. 2016;22(20):5030–5042. https://doi.org/10.1158/1078-0432.CCR-16-0452
8. Srirangam Nadhamuni V, Korbonits M. Novel insights into pituitary tumorigenesis: genetic and epigenetic mechanisms. *Endocr Rev*. 2020;41(6):821–846. https://doi.org/10.1210/endrev/bnaa006
9. Iglesias P, Magallón R, Mitjavila M, Rodríguez Berrocal V, Pian H, Díez JJ. Multimodal therapy in aggressive pituitary tumors. *Endocrinol Diabetes Nutr*. 2020;67(7):469–485. https://doi.org/10.1016/j.endinu.2019.08.004
10. Raverot G, Ilie MD, Lasolle H, et al. Aggressive pituitary tumours and pituitary carcinomas. *Nat Rev Endocrinol*. 2021;17(11):671–684. https://doi.org/10.1038/s41574-021-00550-w
11. Fougner SL, Lekva T, Borota OC, Hald JK, Bollerslev J, Berg JP. The expression of E-cadherin in somatotroph pituitary adenomas is related to tumor size, invasiveness, and somatostatin analog response. *J Clin Endocrinol Metab*. 2010;95(5):2334–2342. https://doi.org/10.1210/jc.2009-2197
12. Lloyd RV, Scheithauer BW, Kuroki T, Vidal S, Kovacs K, Stefaneanu L. Vascular endothelial growth factor (VEGF) expression in human pituitary adenomas and carcinomas. *Endocr Pathol*. 1999;10(3):229–235. https://doi.org/10.1007/BF02738884
13. Vierimaa O, Georgitsi M, Lehtonen R, et al. Pituitary adenoma predisposition caused by germline mutations in the AIP gene. *Science*. 2006;312(5777):1228–1230. https://doi.org/10.1126/science.1126100
14. Uraki S, Ariyasu H, Doi A, et al. Atypical pituitary adenoma with MEN1 somatic mutation associated with abnormalities of DNA mismatch repair genes; MLH1 germline mutation and MSH6 somatic mutation. *Endocr J*. 2017;64(9):895–906. https://doi.org/10.1507/endocrj.EJ17-0036
15. Trivellin G, Daly AF, Faucz FR, et al. Gigantism and acromegaly due to Xq26 microduplications and *GPR101* mutation. *N Engl J Med*. 2014;371(25):2363–2374. https://doi.org/10.1056/NEJMoa1408028
16. Casar-Borota O, Boldt HB, Engström BE, et al. Corticotroph aggressive pituitary tumors and carcinomas frequently harbor ATRX mutations. *J Clin Endocrinol Metab*. 2021;106(4):e1183–e1194. https://doi.org/10.1210/clinem/dgaa749

17. Portovedo S, Neto LV, Soares P, Carvalho DP de, Takiya CM, Miranda-Alves L. Aggressive nonfunctioning pituitary neuroendocrine tumors. *Brain Tumor Pathol*. 2022;39(4):183–199. https://doi.org/10.1007/s10014-022-00441-6
18. Puig-Domingo M, Gil J, Sampedro-Nuñez M, et al. Molecular profiling for acromegaly treatment: a validation study. *Endocr Relat Cancer*. 2020;27(6):375–389. https://doi.org/10.1530/ERC-18-0565
19. Gluenz E, Höög JL, Smith AE, Dawe HR, Shaw MK, Gull K. Beyond 9+0: noncanonical axoneme structures characterize sensory cilia from protists to humans. *FASEB J Off Publ Fed Am Soc Exp Biol*. 2010;24(9):3117–3121. https://doi.org/10.1096/fj.09-151381
20. Fabbri L, Bost F, Mazure NM. Primary cilium in cancer hallmarks. *Int J Mol Sci*. 2019;20(6), E1336. https://doi.org/10.3390/ijms20061336
21. Liu H, Kiseleva AA, Golemis EA. Ciliary signalling in cancer. *Nat Rev Cancer*. 2018;18(8):511–524. https://doi.org/10.1038/s41568-018-0023-6
22. Hassounah NB, Bunch TA, McDermott KM. Molecular pathways: the role of primary cilia in cancer progression and therapeutics with a focus on hedgehog signaling. *Clin Cancer Res*. 2012;18(9):2429–2435. https://doi.org/10.1158/1078-0432.CCR-11-0755
23. Rohatgi R, Milenkovic L, Scott MP. Patched1 regulates hedgehog signaling at the primary cilium. *Science*. 2007;317(5836):372–376. https://doi.org/10.1126/science.1139740
24. May-Simera HL, Kelley MW. Cilia, Wnt signaling, and the cytoskeleton. *Cilia*. 2012;1(1):7. https://doi.org/10.1186/2046-2530-1-7
25. Schneider L, Clement CA, Teilmann SC, et al. PDGFRalphaalpha signaling is regulated through the primary cilium in fibroblasts. *Curr Biol CB*. 2005;15(20):1861–1866. https://doi.org/10.1016/j.cub.2005.09.012
26. Eguether T, Hahne M. Mixed signals from the cell's antennae: primary cilia in cancer. *EMBO Rep*. 2018;19(11):e46589. https://doi.org/10.15252/embr.201846589
27. O'Toole SM, Chapple JP. Primary cilia: a link between hormone signalling and endocrine-related cancers? *Biochem Soc Trans*. 2016;44(5):1227–1234. https://doi.org/10.1042/BST20160149
28. Iwanaga T, Hozumi Y, Takahashi-Iwanaga H. Immunohistochemical demonstration of dopamine receptor D2R in the primary cilia of the mouse pituitary gland. *Biomed Res Tokyo Jpn*. 2011;32(3):225–235. https://doi.org/10.2220/biomedres.32.225
29. Yuan K, Frolova N, Xie Y, et al. Primary cilia are decreased in breast cancer: analysis of a collection of human breast cancer cell lines and tissues. *J Histochem Cytochem Off J Histochem Soc*. 2010;58(10):857–870. https://doi.org/10.1369/jhc.2010.955856
30. Egeberg DL, Lethan M, Manguso R, et al. Primary cilia and aberrant cell signaling in epithelial ovarian cancer. *Cilia*. 2012;1(1):15. https://doi.org/10.1186/2046-2530-1-15
31. Hassounah NB, Nagle R, Saboda K, Roe DJ, Dalkin BL, McDermott KM. Primary cilia are lost in preinvasive and invasive prostate cancer. *PloS One*. 2013;8(7). https://doi.org/10.1371/journal.pone.0068521. e68521-e68521.
32. Lee J, Yi S, Kang YE, et al. Defective ciliogenesis in thyroid hürthle cell tumors is associated with increased autophagy. *Oncotarget*. 2016;7(48):79117–79130. https://doi.org/10.18632/oncotarget.12997
33. Nishioka H, Inoshita N. New WHO classification of pituitary adenomas (4th edition): assessment of pituitary transcription factors and the prognostic histological factors. *Brain Tumor Pathol*. 2018;35(2):57–61. https://doi.org/10.1007/s10014-017-0307-7
34. Villa C, Vasiljevic A, Jaffrain-Rea ML, et al. A standardised diagnostic approach to pituitary neuroendocrine tumours (PitNETs): a European Pituitary Pathology Group (EPPG) proposal. *Virchows Arch Int J Pathol*. 2019;475(6):687–692. https://doi.org/10.1007/s00428-019-02655-0
35. Barry S, Carlsen E, Marques P, et al. Tumor microenvironment defines the invasive phenotype of AIP-mutation-positive pituitary tumors. *Oncogene*. 2019;38(27):5381–5395. https://doi.org/10.1038/s41388-019-0779-5
36. Neou M, Villa C, Armignacco R, et al. Pangenomic classification of pituitary neuroendocrine tumors. *Cancer Cell*. 2020;37(1):123–134.e5. https://doi.org/10.1016/j.ccell.2019.11.002
37. Yu G, Wang LG, Han Y, He QY. clusterProfiler: an R package for comparing biological themes among gene clusters. *Omics J Integr Biol*. 2012;16(5):284–287. https://doi.org/10.1089/omi.2011.0118
38. Ashburner M, Ball CA, Blake JA, et al. Gene ontology: tool for the unification of biology. The Gene Ontology Consortium. *Nat Genet*. 2000;25(1):25–29. https://doi.org/10.1038/75556
39. Kanehisa M. KEGG: Kyoto Encyclopedia of Genes and Genomes. *Nucleic Acids Res*. 2000;28(1):27–30. https://doi.org/10.1093/nar/28.1.27
40. Gillespie M, Jassal B, Stephan R, et al. The reactome pathway knowledgebase 2022. *Nucleic Acids Res*. 2022;50(D1):D687–D692. https://doi.org/10.1093/nar/gkab1028
41. Horvath E. Ultrastructural markers in the pathologic diagnosis of pituitary adenomas. *Ultrastruct Pathol*. 1994;18(1-2):171–179. https://doi.org/10.3109/01913129409016287
42. Horvath E, Kovacs K. Ultrastructural classification of pituitary adenomas. *Can J Neurol Sci J Can Sci Neurol*. 1976;3(1):9–21. https://doi.org/10.1017/s0317167100025944
43. Horvath E, Kovacs K. Ultrastructural diagnosis of human pituitary adenomas. *Microsc Res Tech*. 1992;20(2):107–135. https://doi.org/10.1002/jemt.1070200202
44. Nevers Y, Prasad MK, Poidevin L, et al. Insights into ciliary genes and evolution from multi-level phylogenetic profiling. *Mol Biol Evol*. 2017;34(8):2016–2034. https://doi.org/10.1093/molbev/msx146
45. Patir A, Fraser AM, Barnett MW, et al. The transcriptional signature associated with human motile cilia. *Sci Rep*. 2020;10(1), 10814. https://doi.org/10.1038/s41598-020-66453-4
46. Tsang WY, Bossard C, Khanna H, et al. CP110 suppresses primary cilia formation through its interaction with CEP290, a protein deficient in human ciliary disease. *Dev Cell*. 2008;15(2):187–197. https://doi.org/10.1016/j.devcel.2008.07.004
47. Wong SY, Seol AD, So PL, et al. Primary cilia can both mediate and suppress Hedgehog pathway-dependent tumorigenesis. *Nat Med*. 2009;15(9):1055–1061. https://doi.org/10.1038/nm.2011
48. Menzl I, Lebeau L, Pandey R, et al. Loss of primary cilia occurs early in breast cancer development. *Cilia*. 2014;3(1):7. https://doi.org/10.1186/2046-2530-3-7
49. Seeley ES, Carrière C, Goetze T, Longnecker DS, Korc M. Pancreatic cancer and precursor pancreatic intraepithelial neoplasia lesions are devoid of primary cilia. *Cancer Res*. 2009;69(2):422–430. https://doi.org/10.1158/0008-5472.CAN-08-1290
50. Basten SG, Willekers S, Vermaat JS, et al. Reduced cilia frequencies in human renal cell carcinomas versus neighboring parenchymal tissue. *Cilia*. 2013;2(1):2. https://doi.org/10.1186/2046-2530-2-2
51. Moser JJ, Fritzler MJ, Rattner JB. Ultrastructural characterization of primary cilia in pathologically characterized human glioblastoma multiforme (GBM) tumors. *BMC Clin Pathol*. 2014;14:40. https://doi.org/10.1186/1472-6890-14-40
52. Moser JJ, Fritzler MJ, Rattner JB. Primary ciliogenesis defects are associated with human astrocytoma/glioblastoma cells. *BMC Cancer*. 2009;9(1):448. https://doi.org/10.1186/1471-2407-9-448
53. Han YG, Kim HJ, Dlugosz AA, Ellison DW, Gilbertson RJ, Alvarez-Buylla A. Dual and opposing roles of primary cilia in medulloblastoma development. *Nat Med*. 2009;15(9):1062–1065. https://doi.org/10.1038/nm.2020
54. Coy S, Du Z, Sheu SH, et al. Distinct patterns of primary and motile cilia in Rathke's cleft cysts and craniopharyngioma subtypes. *Mod Pathol Off J U S Can Acad Pathol Inc*. 2016;29(12):1446–1459. https://doi.org/10.1038/modpathol.2016.153
55. Horvath E, Kovacs K, Penz G, Ezrin C. Origin, possible function and fate of "follicular cells" in the anterior lobe of the human pituitary. *Am J Pathol*. 1974;77(2):199–212.
56. Zhao H, Khan Z, Westlake CJ. Ciliogenesis membrane dynamics and organization. *Semin Cell Dev Biol*. 2023;133:20–31. https://doi.org/10.1016/j.semcdb.2022.03.021
57. Breslow DK, Holland AJ. Mechanism and regulation of centriole and cilium biogenesis. *Annu Rev Biochem*. 2019;88(1):691–724. https://doi.org/10.1146/annurev-biochem-013118-111153
58. Sarkisian MR, Siebzehnrubl D, Hoang-Minh L, et al. Detection of primary cilia in human glioblastoma. *J Neurooncol*. 2014;117(1):15–24. https://doi.org/10.1007/s11060-013-1340-y
59. Massinen S, Hokkanen ME, Matsson H, et al. Increased expression of the dyslexia candidate gene DCDC2 affects length and signaling of primary cilia in neurons. *PloS One*. 2011;6(6):e20580. https://doi.org/10.1371/journal.pone.0020580
60. Jenks AD, Vyse S, Wong JP, et al. Primary cilia mediate diverse kinase inhibitor resistance mechanisms in cancer. *Cell Rep*. 2018;23(10):3042–3055. https://doi.org/10.1016/j.celrep.2018.05.016
61. Villa C, Baussart B, Assié G, Raverot G, Roncaroli F. The World Health Organization classifications of pituitary neuroendocrine tumours: a clinicopathological appraisal. *Endocr Relat Cancer*. 2023;30(8):e230021. https://doi.org/10.1530/ERC-23-0021
62. Trouillas J, Jaffrain-Rea ML, Vasiljevic A, Raverot G, Roncaroli F, Villa C. How to classify the pituitary neuroendocrine tumors (PitNET)s in 2020. *Cancers*. 2020;12(2), E514. https://doi.org/10.3390/cancers12020514
63. Manojlovic-Gacic E, Engström BE, Casar-Borota O. Histopathological classification of non-functioning pituitary neuroendocrine tumors. *Pituitary*. 2018;21(2):119–129. https://doi.org/10.1007/s11102-017-0855-1